

Photocatalytic degradation of malachite green dye using doped and undoped ZnS nanoparticles

Jyoti V. Tolia^{1,2}, Mousumi Chakraborty^{2*} and Z. V. P. Murthy^{2*}

¹ Gujarat Technological University, Department of Chemical Engineering, V. V. P. Engineering College, Rajkot 360005, India

² S. V. National Institute of Technology, Department of Chemical Engineering, Surat 395007, India

*Corresponding authors: e-mail: zvp2000@yahoo.com, zvp2000@ched.svnit.ac.in (Z.V.P. Murthy); mch@ched.svnit.ac.in (Mousumi Chakraborty)

In the present study, ZnS nanoparticles were prepared using the mechanochemical method. The ZnS nanoparticles prepared were doped with different concentrations of manganese using metal acetate and manganese acetate by mechanochemical method. The as-prepared particles were characterized using X-ray diffraction (XRD) and transmission electron microscopy (TEM). The photocatalytic activity of the prepared nanoparticles samples, in the photocatalytic degradation of malachite green, had been investigated. The nanoparticles were photo induced, generating hole transfer for photocatalytic activity. The photodegradation of malachite green was observed at different pH (2–5) values, dye concentrations (10–100 mg/L) and amount of ZnS nanoparticles (1–2.5 g/L). About 95% degradation of dye was observed on the addition of 2 g/L ZnS in 50 mg/L dye solution after 90 minutes illumination at 125 W. Degradation has been increased up to 99% using UV/nanoparticles/H₂O₂ (50 mL/L) combined process. The degradation efficiency was also compared using Mn doped ZnS nanoparticles (Zn_{1-x}Mn_xS, where $x = 0.01, 0.22$ and 0.3). Maximum of 97% degradation was observed with 0.01% concentration of Mn. Kinetics study and performance of UV/ZnS, UV/ZnS/H₂O₂, UV/doped ZnS processes were evaluated to compare the efficiency of different processes.

Keywords: Mechanochemical method, advanced oxidation process, photocatalytic degradation, malachite green, nanoparticles.

INTRODUCTION

At present, a large part of pollution in the public water systems is caused by the industries. Among the chemical contaminants, dyes and dyes intermediates, surfactants and some traces of metals are the objects of major interest in the preservation of the environment. About 10–15% of all the dyes are directly lost to wastewater in the dyeing process. Thus, the wastewater must be treated before releasing it into the natural environment¹⁻². These dyes create serious environmental hazards and pollution by releasing toxic and potential carcinogenic substances into the aqueous phase³⁻⁵. Various chemical and physical processes, such as chemical precipitation, coagulation, electrocoagulation, adsorption, air stripping, flocculation, ozonation, chlorination, ultrafiltration, reverse osmosis, etc., are applied for colour removal from textile effluents. But these processes lead to non-biodegradable contaminations which give rise to new types of pollutants and need to be further treated^{3-4,6-7}. One such textile effluent is malachite green (MG). Several research works have been reported for MG degradation, using biosorption onto wheat bran, hen feathers and micro algae *Cosmarium* sp.⁸⁻¹⁰, ultrasonic irradiation¹¹, and sunlight irradiation¹². But, recently advanced oxidation processes (AOPs) have emerged as promising option for the removal of MG from wastewaters. In the AOPs complete organic matter mineralization can be achieved. The variety of AOPs comes from the fact that there are many ways for hydroxyl radical production. Above all, it should be taken into account that these AOPs are brought into use with the application of semiconductors, light and some reactants, viz., H₂O₂, UV and/or O₃, etc¹³. In photocatalysis process, under UV irradiation, semiconductor particles absorb photon of light more energetic than its band gap. In this

circumstance, the electrons in semiconductor materials get excited from the valence band to conduction band and generate charge carriers (electrons/holes). These charge carriers (holes) are responsible for the oxidation and formation of hydroxyl radicals¹⁴. The hydroxyl radical possesses inherent properties that enable it to attack refractory organic pollutants in water to possibly obtain a complete mineralization¹⁵. Compared to other semiconductor photocatalysts, TiO₂ has so far been shown to be the most promising material used for both fundamental research and practical applications because it is highly photoreactive, cheap, non-toxic, chemically and biologically inert, and photostable¹⁶. Metal sulfides are visible light responsive photocatalysts because valence band of the metal sulfides consists of 3p orbital of S, which results in a more occupied valence band and narrower band gap as compared to metal oxides. In many studies metal sulfides like ZnS and CdS have been focused as photocatalysts¹⁷⁻¹⁹. Zinc sulphide is one of the semiconductor nanomaterials that can be used for the production of optical sensitizers, photocatalysts, electroluminescent materials, optical sensors and for solar energy conversion²⁰.

In the present work degradation of malachite green dye was studied using doped and undoped ZnS nanoparticles with the combination of different processes, viz., UV/ZnS, UV/ZnS/H₂O₂ and UV/doped ZnS. The effects of the operating parameters, like pH, catalyst loading and initial dye concentration on degradation rate were also evaluated. Finally, kinetics study was also performed by varying operating conditions of the system.

EXPERIMENTAL

Materials and methods

Zinc acetate and manganese acetate (S.D. Fine Chemicals, Mumbai, India), sodium sulfide (Loba Chemicals, Mumbai, India) and malachite green (Himedia, Mumbai, India) of analytical grade were directly used without further purification. Hydrogen peroxide (30%w/w), NaOH and HCl were purchased from S.D. Fine Chemicals, Mumbai, India. The solutions were prepared by dissolving the requisite amount of dye in double distilled water for each experiment.

Testing equipment

The powder X-ray diffraction (XRD) analysis was made using diffractometer X'Pert (Philips, The Netherlands) with CuK α radiation ($\lambda=1.5418$ Å). The morphology of ZnS nanoparticles was observed by transmission electron microscopy (TEM) using a transmission electron microscope (Technai-20, 200KV, Phillips, The Netherlands). The absorption spectra were analyzed at different time intervals using a UV-Vis spectrophotometer (HACH, Germany). The effect of pH was measured using a pH meter NIG 334 (Biocraft, India).

Synthesis of undoped ZnS and Mn doped ZnS photocatalyst

ZnS nanoparticles were synthesized by mechanochemical process using zinc acetate and sodium sulfide in molar ratio of 1.2:1²¹⁻²². The reactants were placed inside a tungsten carbide bowl under high purity air atmosphere in a planetary ball mill (FRITSCH's "Pulverisette 6", Germany) for a period of 8h. The milling speed was set at 350 rpm with steel balls (diameter = 1mm). The obtained ZnS nanoparticles were washed 3–4 times with distilled water, then water soluble sodium acetate and excess metal acetate were decanted. The particles were then dried and characterized. Similarly, zinc acetate and manganese acetate mixtures (different proportions) were used to synthesize Mn-doped ZnS by mechanochemical process.

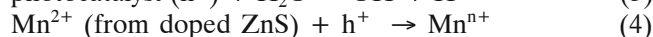
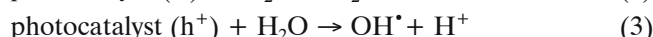
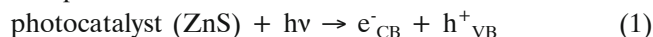
Photocatalytic degradation experiments

The photocatalytic degradation experiments were performed in a cylindrical quartz glass reactor of 250mL. The UV irradiation was achieved through quartz by using UV lamp of 125W (medium pressure lamp), which was provided with cooling water. The reactor was filled with the dye solution placed between the reactor walls and UV lamp system. The effect of dye adsorption was studied by adjusting pH in the range 2–5 by adding appropriate amount of HCl and/or NaOH in a series of experiments. The adsorption of dye on the photocatalyst was allowed for fixed time (30 minutes) in dark environment with a continuous stirring so that no degradation would take place before UV irradiation. The photocatalyst of 1 g/L was freely suspended and the dye solution (25g/L) was stirred with UV irradiation for 90 minutes to study the effect of pH in the range 2–5. Initially the pH was optimized and the remaining experiments were performed to study the effects of dye concentration, catalyst dosing and volume of hydrogen peroxide. The initial sample at time zero was taken when the light source was switched

on along with water pumping. Samples from the reactor were taken at every 15 minutes and analyzed immediately to avoid any further reaction. The concentration change in dye was observed using the spectrophotometer.

Mechanism for photocatalytic degradation

The photocatalytic process is initiated by the illumination of semiconductor photocatalyst using high energy photon of UV irradiation. These photons have energy greater than band gap energy of semiconductor photocatalyst. This generates electrons and holes from conduction and valence band. The degradation mechanism is explained below:



RESULTS AND DISCUSSION

Characterization of photocatalyst

The undoped and Mn-doped ZnS photocatalysts prepared by mechanochemical method were characterized using XRD. The XRD analysis shown in Fig. 1(a) revealed hexagonal wurzite α -ZnS (JCPDS 72-0163) together with cubic spherulite β -ZnS (JCPDS 5-0566) as the only products of mechanochemical synthesis. Thus, the crystal was polymorph of zinc blend as XRD pattern also had few peaks of wurtzite. The coexistence

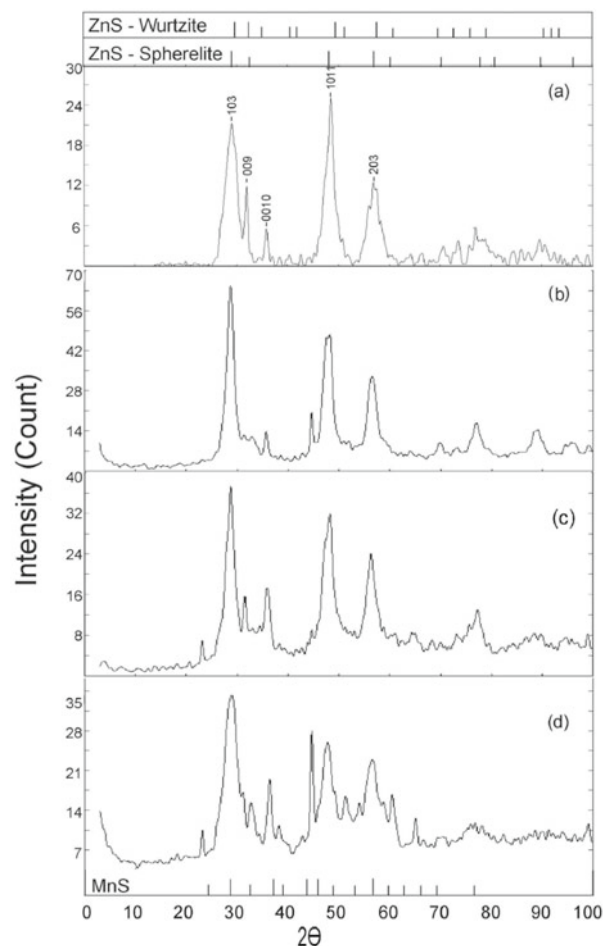


Figure 1. XRD of ZnS (a) and Zn_{1-x}Mn_xS, where x= 0.01(b), 0.22(c) and 0.3(d)

of both phases was also reported in literature^{23,24}, which indicated phase transformation as the consequence of the motion of dislocations in the activated solid state. The spectra were matched for various diffraction peaks at 2θ values of 29.03° , 48.49° and 56.87° corresponding to the diffraction planes (103), (1011) and (203), respectively, for wurzite ZnS. Similarly, the peaks were also found to match at 28.792° , 48.121° and 56.874° corresponding to the diffraction planes (111), (220) and (311), respectively, for cubic ZnS. It was found that the peaks at higher angles matched with wurtzite phase. The observations showed that the intensities of the peaks steadily became weaker (except at $2\theta = 29.03^\circ$) with increasing 2θ angle and also the major intense peaks were wider and the broad hump (and therefore large FWHM) suggested that the synthesized materials were nanocrystalline in nature with very small particle size. Hence, the average particle size was calculated using Scherrer formula²⁵ and it was found to be 4.79 nm, which is in consistence with TEM image (Fig. 2). The XRD patterns shown in Fig. 1(b,c,d) of the ZnS:Mn nanocrystals showed very broad diffraction peaks (at 2θ values of 35.734° , 36.375° and 35.953°) with increasing concentration of manganese ($\text{Zn}_{1-x}\text{Mn}_x\text{S}$, where $x = 0.01, 0.22$ and 0.3 , respectively), which was the characteristic of nanosized material. For all the samples, the three main diffraction peak positions correspond to the lattice planes of (111), (220) and (311) were matching the cubic zinc blend ZnS structure (JCPDS No: 05-0566).

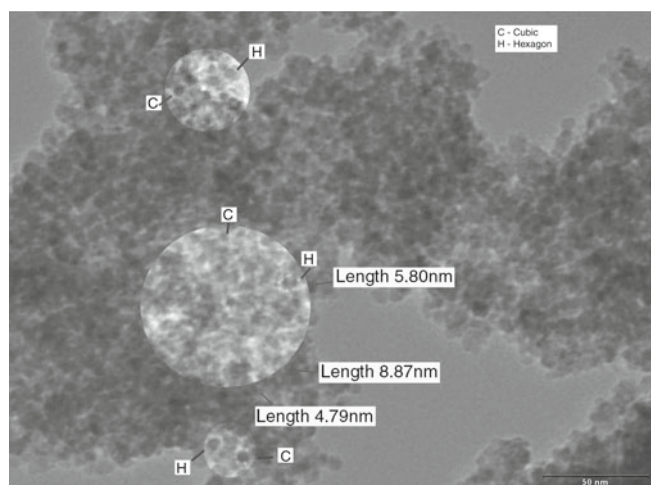


Figure 2. TEM image of ZnS nanoparticle

Effect of pH

Literature review revealed that pH played a significant role in the degradation and had shown variation in its effect for different ranges^{2,4,26}. The samples at different pH were analyzed and percentage degradation of malachite green was found to be 60, 60, 72 and 56% at pH 2, 3, 4 and 5, respectively. Fig. 3 indicated that degradation of malachite green was greatly influenced by pH of the dye solution. The degradation efficiency increased from 60 to 72% as a consequence of increase in pH from 2 to 4, respectively. The pH affected surface binding sites of the adsorbent (anionic dye solution) as well as the availability of the adsorbate compound (cationic photocatalyst). Malachite green, with anionic configuration, showed favorable adsorption in acidic solution²⁷. At acidic pH the photocatalyst surface was

positively charged and hence attracted the negatively charged dye solution. But at $\text{pH} > 4$, (i.e., at $\text{pH} = 5$) the photocatalytic degradation was found to decrease. This was because at $\text{pH} > 4$, the dye uptake was high and there was a complete coverage of the catalyst surface by dye molecules, which made the catalyst surface slightly anionic/negatively charged. Such a strong adsorption of dye molecules led to a major decrease of the active sites and consequently a decrease in the absorbed light on the catalyst's surface, which lead to decrease in degradation rate²⁸. This prohibited the adsorption of H_2O or OH^- on the surface and inhibited the initial process of formation of the reactive hydroxyl radicals responsible for degradation. Thus, the surface charge on photocatalyst affected the degradation reaction when it was positive. A similar trend of dye adsorption in acidic medium was observed by Mittal²⁶ at $\text{pH} = 5$. After a particular pH, the net charge on semiconductor surface became zero and was called point of zero discharge (pzc). Gandhi *et al.*²⁹ also observed maximum degradation of MG dye in acidic pH using ZnS-CdS as a photocatalyst. Among the studied pH range, the electrostatic interaction between catalyst surface and dye molecule was maximum at 4 and hence all other experiments were performed at pH 4.

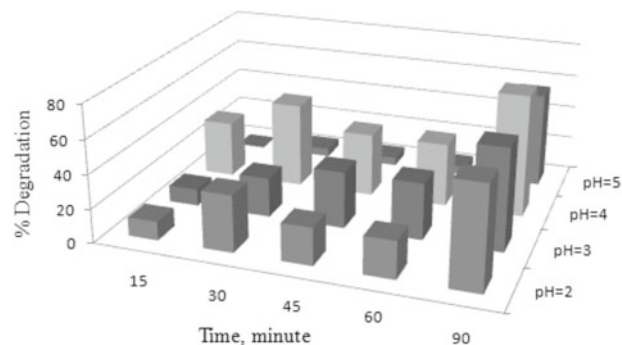


Figure 3. Effect of dye adsorption time and pH

Effect of initial dye concentration

The effect of dye concentration on the rate of the reaction of photocatalytic degradation was studied. It had been observed that on increasing the initial dye concentration from 10–100 mg/L, the degradation efficiency after 90 minutes of irradiation was found to be 30, 32, 80 and 35% for dye solution of 10, 25, 50 and 100 mg/L, respectively. It can be observed that the degradation efficiency has increased to maximum at 50 mg/L initial dye concentration and decreased with further increase. Initially, the catalyst surface area available helped to increase degradation efficiency but with a further increase of dye concentration (above 50 mg/L) active sites of the catalyst were fully occupied by dye molecules and no space was available for OH^\bullet radicals generation. The high concentration of dye would have acted as a filter for the incident light, which ultimately reduced degradation efficiency^{5,30}.

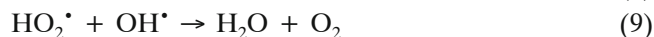
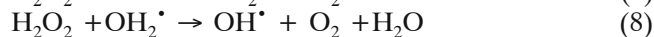
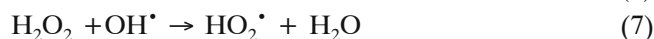
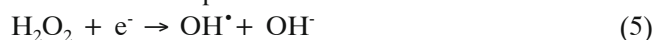
Effect of catalyst loading

To determine the effect of catalyst loading on the reaction rate, several experiments were conducted at catalyst loading from 1.0–2.5 g/L (at optimum conditions of $\text{pH} = 4$ and dye concentration = 50 mg/L). The degradation rate increased with increasing the loading of the photocatalyst up to 2 g/L (95% degradation) provid-

ing large surface area for photodegradation. In general, the greater the amount of the photocatalyst, the higher the rate of reaction due to increased active sites of the photocatalyst^{3,5} would be. However, at the same time more photocatalyst would also have induced greater aggregation, which resulted in the decrease in the surface area of the photocatalyst, making a significant fraction of the catalyst to be inaccessible to adsorbing the dye^{3,5}. Besides this, the degradation rate constant decreased after an optimum value for the photocatalyst loading as in the concentration of dye, the opacity of dye solution also increased and UV radiation got scattered reducing the optical path. In these conditions, the penetration depth of the photon was decreased and fewer catalyst nanoparticles could be activated⁵.

Effect of H₂O₂ concentration

UV irradiation of MG dye at optimum conditions (pH = 4, dye concentration = 50 mg/L and catalyst dose = 2 g/L) was carried out for 90 minutes using different concentrations of H₂O₂ in the range 40–200 mL/L. H₂O₂ produces highly reactive hydroxyl radicals, which were responsible for degradation of dye. The maximum removal efficiency (99%) was obtained at 100 mL/L of H₂O₂ concentration, and it slightly decreased above 100 mL/L because highly reactive hydroxyl radicals reacted with excess amount of H₂O₂ and produced hydroperoxyl radicals (HO₂•)^{6–7,31–32}, which were less reactive and ultimately inhibited the degradation³¹. The reaction mechanism is explained below:



Effect of manganese doping

In order to study the effect of dopant on degradation efficiency, photodegradation experiments were carried out in the presence of UV irradiation with doped catalysts for 90 minutes. The degradation efficiency was found to be 97, 96 and 96% for Zn_{1-x}Mn_xS, where x = 0.01, 0.22

and 0.3, respectively. Doping ions offered a way to trap electrons and/or holes on the surface or during interface charge transfer because of the different positions of the dopant in the host lattice. The semiconductor hole is a positively charged one and an electron acceptor. It is an oxidizing agent that, by virtue of its accepting electrons, is itself reduced in the process. The holes are generated from ZnS semiconductor due to illumination on its (catalyst) surface. These holes oxidise the Mn²⁺ ion to higher oxidation state (n = +4, +6 and +7) ion (as per equations 1–4). Due to the loss of an electron, the resulting ion goes to a higher energy level and it becomes a strong oxidizing agent for dyes. As a result, in these conditions, apart from holes and hydroxyl radicals generated by photocatalyst, Mn ion (at higher oxidation state) also acts as an oxidizing agent and therefore, the rate of decolorization was found to be increased. But it was also found that with increasing the doping concentration, photodegradation efficiency decreases because the increase in manganese ions will replace Zn ions in ZnS lattice structure and forms MnS, which will reduce the activity of trapping electrons/holes.

It was found that with increasing the doping concentration, photodegradation efficiency decreased because the increase in manganese ions would replace Zn ions in ZnS lattice structure which would reduce the activity of the trapping electrons/holes²⁶.

Kinetic studies and comparison among different processes

Degradation of MG was carried out using the optimum conditions (irradiation time of 90 minutes, pH=4, dye concentration=50 mg/L, catalyst loading=2 g/L, H₂O₂ concentration=100 mL/L and doping concentration, x=0.01 Mn) for different combinations of processes (UV/ZnS, UV/ZnS/H₂O₂ and UV/Mn doped ZnS). The MG degradation was observed as a function of irradiation time and data were used for fitting with different rate models. The fitting with the first-order-rate model; ln C/C₀ versus time was ruled out as the plot was found to be curved. The linear plot of t/C versus time (equation 10) was found to match pseudo-second-order rate model³³:

$$\frac{t}{C} = \frac{1}{k_{\text{app}}C_0^2} + \frac{1}{C_0}t \quad (10)$$

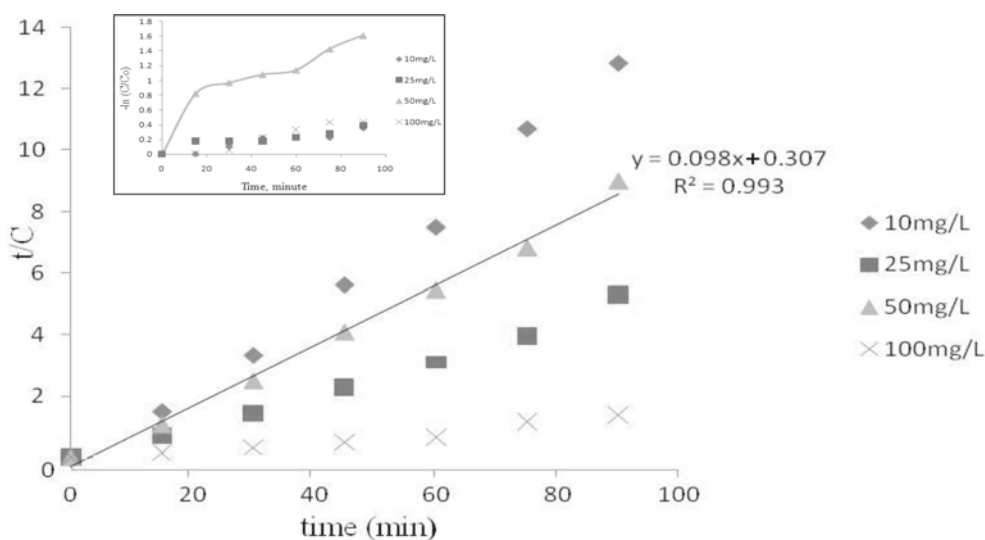


Figure 4a. Pseudo-second-order kinetics of UV/ZnS process with inset showing first order kinetics

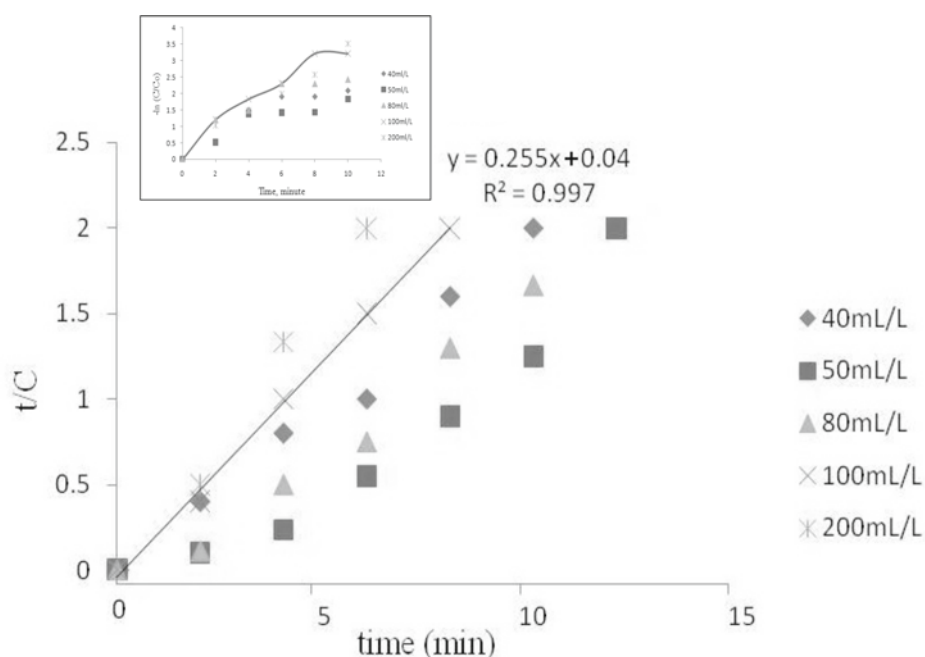


Figure 4b. Pseudo-second-order kinetics of UV/ZnS/H₂O₂ process with inset showing first order kinetics

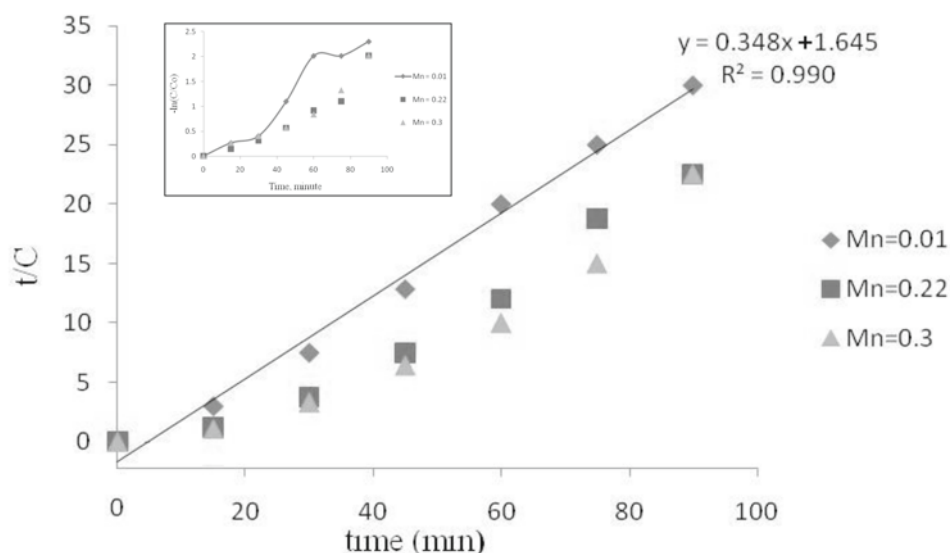


Figure 4c. Pseudo-second-order kinetics of UV/doped ZnS process with inset showing first order kinetics

where, C_0 and C are the concentrations of dye at irradiation time $t = 0$ and $t = t$, respectively, k_{app} is the apparent rate constant obtained from the intercept. The possible explanation for pseudo-second-order could be the formation of some intermediate compounds and dimer^{20,34}. Amongst the different processes, the combined process of UV/ZnS/H₂O₂ showed the highest percentage degradation (Fig. 4(b)) compared to the other processes used ((Fig. 4(a) and 4(c)). The rate constants for UV/ZnS and UV/doped ZnS were found to be 0.031 min^{-1} and 0.073 min^{-1} , respectively. The application of both the oxidant (H₂O₂) and photocatalyst enhanced the degradation rate and provided maximum degradation efficiency (99%) and highest rate constant (1.62 min^{-1}) value.

CONCLUSIONS

The study showed the potential of photocatalytic degradation in water purification. Out of different processes employed, a significant enhancement of the photocatalytic

activity was observed in the system using a combination of oxidant and photocatalyst irradiation under UV light. Concentration of both the oxidant and the photocatalyst greatly influenced the degradation rate. Also, the process was observed to be strongly pH dependent. The degradation followed pseudo-second-order kinetics. Photodegradation could be a recommended approach for the treatment of wastewaters containing malachite green dye as pollutant. Keeping in view all the factors, it may be said that the combined system is an efficient one amongst all other processes.

LITERATURE CITED

1. Parshetti, G., Kalme, S., Saratale, G. & Govindwar, S. (2006). Biodegradation of malachite green by *Kocuria rosea* MTCC 1532. *Acta Chim. Slov.* 53, 492–498.
2. Oturan, M.A., Guivarch, E., Oturan, N. & Sires, I. (2008). Oxidation pathways of malachite green by Fe³⁺-catalyzed electro-Fenton process. *Appl. Catal. B: Environ.* 82, 244–254. DOI: 10.1016/j.apcatb.2008.01.016.

3. Kansal, S.K., Singh, M. & Sud, D. (2007). Studies on photodegradation of two commercial dyes in aqueous. *J. Hazard. Mater.* 141, 581–590. DOI: 10.1016/j.jhazmat.2006.07.035.
4. Hachem, C., Bocquillon, F., Zahraa, O. & Bouchy, M. (2001). Decolourization of textile industry wastewater by the photocatalytic degradation process. *Dyes Pigments*. 49, 117–125.
5. Barjasteh-Moghaddam, M. & Habibi-Yangjeh, A. (2011). Effect of operational parameters on photodegradation of methylene blue on ZnS nanoparticles prepared in presence of an ionic liquid as a highly efficient photocatalyst. *J. Iran. Chem. Soc.* 8, S169–S175.
6. Sayilkan, F., Asilturk, M., Tatar, P., Kiraz, N., Arpac, E. & Sayilkan, H. (2007). Photocatalytic performance of Sn-doped TiO₂ nanostructured mono and double layer thin films for malachite green dye degradation under UV and vis-lights. *J. Hazard. Mater.* 144, 140–146. DOI: 10.1016/j.jhazmat.2006.10.011.
7. Modirshahla, N. & Behnajady, M.A. (2006). Photooxidative degradation of malachite green (MG) by UV/H₂O₂: Influence of operational parameters and kinetic modeling. *Dyes Pigments* 70, 54–59. DOI: 10.1016/j.dyepig.2005.04.012.
8. Paninutti, L., Mouso, N. & Forchiassin, F. (2006). Removal and degradation of the fungicide dye malachite green from aqueous solution using the system wheat bran-Fomes sclerodermeus. *Enzyme Microb. Technol.* 39, 848–853. DOI: 10.1016/j.enzmictec.2006.01.013.
9. Sambasivam, S., Joseph, D.P., Reddy, D.R., Reddy, B.K. & Jayasankar, C.K. (2008). Synthesis and characterization of thiophenol passivated Fe doped ZnS nanoparticles. *Mater. Sci. Eng.*, B. 150, 125–129. DOI: 10.1016/j.mseb.2008.03.009.
10. Daneshwar, N., Ayazloo, M., Khataee, A.R. & Pourhassan, M. (2007). Biological decolorization of dye solution containing malachite green by microalgae *Cosmarium* sp. *Bioresour. Technol.* 98, 1176–1182. DOI: 10.1016/j.biortech.2006.05.025.
11. Behnajady, M., Modirshahla, N., Shokri, M. & Vahid, B. (2008). Effect of operational parameters on degradation of malachite green by ultrasonic irradiation. *Ultrason. Sonochem.* 15, 1009–1014. DOI: 10.1016/j.ultrasonch.2008.03.004.
12. Pérez-Estrada, L.A., Agüera, A., Hernando, M.D., Malato, S. & Fernández-Alba, A.R. (2008). Photodegradation of malachite green under natural sunlight irradiation: Kinetic and toxicity of the transformation products. *Chemosphere*. 70, 2068–2075. DOI: 10.1016/j.chemosphere.2007.09.008.
13. Oussi, D., Mokriani, A. & Esplugas, S. (1997). Removal of aromatic compounds using UV/H₂O₂. *Trends Photochem. Photobiol.* 1, 77–83.
14. Carlos, G.A.K., Fernando, W., Sandra, M.G., Nelson, D., Noemi, N. & Patricio, P.Z. (2000). Semiconductor-assisted photocatalytic degradation of reactive dyes in aqueous solution. *Chemosphere*. 40, 433–440.
15. Wen, K.S. & Li, W.N. (2010). Fenton degradation of 4-chlorophenol contaminated water promoted by solar irradiation. *Solar Energy* 84, 59–65. DOI: 10.1016/j.solar.2009.10.006.
16. Nagaveni, K., Sivalingam, G., Hegde, M.S. and Giridhar, M. (2004). Solar photocatalytic degradation of dyes: high activity of combustion synthesized nano TiO₂. *Appl. Catal. B: Environ.* 48, 83–93. DOI: 10.1016/j.apcatb.2003.09.013.
17. Colmenares, J.C., Luque, R., Campelo, J.M., Colmenares, F., Karpiński, Z. & Romero, A.A. (2009). Nanostructured photocatalysts and their applications in the photocatalytic transformations of lignocellulosic biomass: An overview. *Materials* 2, 2228–2258. DOI: 10.3390/ma2042228.
18. Yang, J., Peng, J.J., Zou, R., Peng, F., Wang, H., Yu, H. and Lee, J.Y. (2008). Mesoporous zinc-blende ZnS nanoparticles: synthesis, characterization and superior photocatalytic properties. *Nanotechnology*. 19, 255603. DOI: 10.1088/0957-4484/19/25/255603.
19. Yao, T., Zhao, Q., Qiao, Z., Peng, F., Wang, H., Yu, H., Chi, C. and Yang, J. (2011). Chemical synthesis, structural characterization, optical properties and photocatalytic activity of ultrathin ZnSe nanorods. *Chem. Eur. J.* 17, 8663–8670. DOI: 10.1002/chem.201003531.
20. El-Kemary M. & El-Shamy, H. (2009). Fluorescence modulation and photodegradation characteristics of safranin O dye in the presence of ZnS nanoparticles, *J. Photochem. Photobiol. A*: 205, 151–155. DOI: 10.1016/j.jphotochem.2009.04.021.
21. Godočikova, E., Criado, J., Real, C. & Gock, E. (2006). Thermal behaviour of mechanochemically synthesized nanocrystalline CuS. *Thermochim. Acta*. 440, 19–22. DOI:10.1016/j.tca.2005.09.015.
22. Tsuzuki, T. & McCormick, P. (2004). Mechanochemical synthesis of nanoparticles. *J. Mater. Sci.* 39, 5143–5146.
23. Geng, B.Y., Liu, X.W., Du, Q.B., Wei, X.W. & Zhang, L.D. (2006). Structure and optical properties of periodically twinned ZnS nanowires. *Appl. Phys. Lett.* 88, 163104-163104-3. DOI: 10.1063/1.2196827.
24. Zhang, Z., Ming, H. & Duan, X. (2009). Optical properties of hexagonal and cubic ZnS nanoribbons: Experiment and theory. *Chinese Phys. Lett.* 26, 066104-1-066104-3.
25. Godocikova, E., Balaz, P., Gock, E., Choi, W. & Kim, B. (2006). Mechanochemical synthesis of the nanocrystalline semiconductors in an industrial mill. *Powder Technol.* 164, 147–152. DOI: 10.1016/j.powtec.2006.03.021.
26. Mittal, A. (2006). Adsorption kinetics of removal of a toxic dye, malachite green, from wastewater by using hen feathers. *J. Hazard. Mater.* 133, 196–202. DOI: 10.1016/j.jhazmat.2005.10.017.
27. Chen, Y., Zhang, Y., Liu, C., Lu, A. and Zhang, W. (2012). Photodegradation of malachite green by nanostructured Bi₂WO₆ visible light induced photocatalyst. *Int. J. Photoenergy*. 2012, 1–6. DOI: 10.1155/2012/510158.
28. Franco, A., Neves, M.C., Ribeiro Carrott, M.M.L., mendonca, M.H., Pereira, M.I. and Monteiro, O.C. (2009). Photocatalytic decolorization of methylene blue in the presence of TiO₂/ZnS composite. *J. Hazard. Mater.* 161, 545–550. DOI: 10.1016/j.jhazmat.2008.03.133.
29. Gandhi, J., Dangi, R., Sharma, J.C., Verma, N. & Bhargwaj, S. (2010). Photocatalytic bleaching of malachite green and brilliant green dyes using ZnS-CdS as semiconductor: A comparative study. *Der Chemica Sinica* 1, 77–83.
30. Pouretedal, H.R., Norozi, A., Keshavarz, M.H. & Semnani, A. (2009). Nanoparticles of zinc sulfide doped with manganese, nickel and copper as nanophotocatalyst in the degradation of organic dyes. *J. Hazard. Mater.* 162, 674–681. DOI: 10.1016/j.jhazmat.2008.05.128.
31. Ghaly, M.Y., Härtel, G., Mayer, R. & Haseneder, R. (2001). Photochemical oxidation of p-chlorophenol by UV/H₂O₂ and photo-Fenton process. A comparative study. *Waste Manage.* 21, 41–47. DOI: 10.1016/S0956-053X(00)00070-2.
32. Aravindhana, R., Fathima, N.N., Rao, J.R. & Nair, B.U. (2006). Wet oxidation of acid brown dye by hydrogen peroxide using heterogeneous catalyst Mn–salen–Y zeolite: A potential catalyst. *J. Hazard. Mater.* 138, 152–159. DOI: 10.1016/j.jhazmat.2006.05.052.
33. Ho, Y.S. and McKay, G. (1999). Pseudo-second order model for sorption processes. *Process Biochem.* 34, 451–465.
34. Muhammad, A.R., Mohammed, A.M., Khaleel, A. & Amal, A. (2010). Photocatalytic degradation of methylene blue using a mixed catalyst and product analysis by LC/MS. *Chem. Eng. J.* 157, 373–378. DOI: 10.1016/j.cej. 2009.11.017.